

Sequence analysis

SNPlice: variants that modulate Intron retention from RNA-sequencing data

Prakriti Mudvari^{1,2,†}, Mercedeh Movassagh^{1,3,†}, Kamran Kowsari^{1,2}, Ali Seyfi^{1,3}, Maria Kokkinaki⁴, Nathan J. Edwards⁶, Nady Golestaneh^{4,5,6} and Anelia Horvath^{1,3,*}

¹McCormick Genomics and Proteomics Center, ²Department of Biochemistry and Molecular Medicine and ³Department of Pharmacology and Physiology, The George Washington University, Washington, DC 20037, USA and ⁴Department of Ophthalmology, ⁵Department of Neurology and ⁶Department of Biochemistry and Molecular & Cellular Biology, Georgetown University, School of Medicine, Washington, DC 20057, USA

*To whom correspondence should be addressed.

[†]The authors wish it to be known that, in their opinion, the first 2 authors should be regarded as Joint First Authors.

Associate Editor: Ivo Hofacker

Received on May 13, 2014; revised on November 3, 2014; accepted on November 30, 2014

Abstract

Rationale: The growing recognition of the importance of splicing, together with rapidly accumulating RNA-sequencing data, demand robust high-throughput approaches, which efficiently analyze experimentally derived whole-transcriptome splice profiles.

Results: We have developed a computational approach, called SNPlice, for identifying cis-acting, splice-modulating variants from RNA-seq datasets. SNPlice mines RNA-seq datasets to find reads that span single-nucleotide variant (SNV) loci and nearby splice junctions, assessing the co-occurrence of variants and molecules that remain unspliced at nearby exon–intron boundaries. Hence, SNPlice highlights variants preferentially occurring on intron-containing molecules, possibly resulting from altered splicing. To illustrate co-occurrence of variant nucleotide and exon–intron boundary, allele-specific sequencing was used. SNPlice results are generally consistent with splice-prediction tools, but also indicate splice-modulating elements missed by other algorithms. SNPlice can be applied to identify variants that correlate with unexpected splicing events, and to measure the splice-modulating potential of canonical splice-site SNVs.

Availability and implementation: SNPlice is freely available for download from <https://code.google.com/p/snplice/> as a self-contained binary package for 64-bit Linux computers and as python source-code.

Contact: pmudvari@gwu.edu or horvatha@gwu.edu

Supplementary information: [Supplementary data](#) are available at *Bioinformatics* online.

1 Introduction

Alternative splicing is well known as an essential mechanism of gene regulation which may affect protein function (Braunschweig *et al.*, 2013; Singh and Cooper, 2012). To date, ~95% of the mammalian genes are estimated to be subjected to alternative splicing; current knowledge explains only a portion of the underlying molecular events (Barash *et al.*, 2010; Bernstein *et al.*, 2012; Moore and Silver,

2008; Pan *et al.*, 2008). Most of the knowledge on the splicing was obtained through alignment of DNA and RNA sequences and systematic search for functional elements, facilitated by the recent advances of the sequencing technologies (Bernstein *et al.*, 2012; Barbosa-Morais *et al.*, 2012; Clark and Thanaraj, 2002; Liao *et al.*, 2005; Merkin *et al.*, 2012). Among the major mechanisms affecting the splicing process are nucleotide changes that disrupt or create

binding sites for splicing, transcriptional and other regulatory factors (Barash *et al.*, 2010; Bernstein *et al.*, 2012; Barbosa-Morais *et al.*, 2012; McManus and Graveley, 2011; Merkin *et al.*, 2012; Moore and Silver, 2008; Pan *et al.*, 2008; Wang and Burge, 2008). In addition to the four consensus sequences critical for the spliceosome assembly—5' splice site (5'SS), 3'SS, the branch sequence, and the polypyrimidine tract (PPT)—changes in the exonic and intronic splicing enhancers and silencers (ESE, ISE, ESS and ISS) and other, less patterned sequences, are increasingly acknowledged as splicing modulators (De Conti *et al.*, 2013; Woolfe *et al.*, 2010). The emerging recognition of the importance of splicing has stimulated efforts for modeling the splice-modulating potential of genetic variants through probabilistic predictions based on junction nucleotide composition, dependencies among neighboring bases, local optimality in the context of the gene structure, homology alignments, interaction with splicing factors and comparison with experimentally verified splice-modulating motifs (Brunak *et al.*, 1991; Brendel and Kleffe, 1998; Dogan *et al.*, 2007; Faber *et al.*, 2011; Kamath *et al.*, 2012; Perteira *et al.*, 2001; Piva *et al.*, 2012; Riva *et al.*, 2012; Woolfe *et al.*, 2010; Yeo and Burge, 2004). These approaches helped annotate numerous previously unknown splice-modulating variants; however, being mostly based on pre-existing knowledge, they may miss variants acting through unknown mechanisms.

Several recent analyses have highlighted the importance of systematic, genome-wide evaluation of sequence-specific splicing events (Barash *et al.*, 2010; Han *et al.*, 2013; Merkin *et al.*, 2012; Sterne-Weiler and Sanford, 2014). A survey of the splicing patterns on relatively small genome portion—250 exons in HapMap-genotyped individuals—has suggested that common splice-modulating SNVs can be frequent in the genome (Cheung *et al.*, 2005; Coulombe-Huntington *et al.*, 2009; Hull *et al.*, 2007). An analysis of splice-sensitive microarrays demonstrated high frequency of alternative splicing events within the usually unexplored areas of the genome, and, at significance levels much below standard multiple-testing thresholds, implying that the extent of cis-regulated differential splicing between individuals may be far greater than estimated (ElSharawy *et al.*, 2009). Concurrent with the above are findings from another study, which employs software—SNPsplicer—to compare matching genomic DNA and complementary DNA (cDNA) from individuals with different genotypes (ElSharawy *et al.*, 2006).

We developed a computational approach, SNPlice, which identifies potential splice-modulating variants from RNA-seq data generated through massively parallel sequencing. SNPlice assesses sequencing reads for co-occurrence of variant base and a nearby exon-intron boundary. Given that canonical splicing is expected to retain predominantly exon-exon junctions in the transcriptome, we based our strategy on the assumption that transcriptome sequencing reads harboring an exon-intron boundary indicate a biological process of junction alteration and, possibly, altered splicing.

2 Methods

2.1 Samples

SNPlice performance was tested on 65 human RNA-seq datasets (Supplementary Table S1). Five in-house primary cell lines derived from Retinal Pigment Epithelia (RPE) of healthy organ donors' eyes (Maminiskis *et al.*, 2006), were used for allele-specific sequencing of selected SNPlice highlighted variants. Sixty matching normal and tumor datasets from the Cancer Genomic Hub (<https://cghub.ucsc.edu>) were used to assess the between-samples variability of SNPlice findings.

2.2 RNA libraries preparation and sequencing

Total RNA from the RPE primary cell lines was isolated using standard protocols (TRIzol Reagent, Life Technologies, Foster City, CA). The libraries were prepared using TruSeq RNA sample preparation kit (Illumina, Inc.) that includes poly-A selection, according to the manufacturer recommendations. Paired-end sequencing (50nt read length) was performed on Illumina HiSeq 2000 platform.

2.3 Read alignment and variants call and annotation

The generated and downloaded sequencing datasets were processed as follows. The paired end raw reads were aligned against hg19 using TopHat2 (Kim *et al.*, 2013), version 2.0.8, with default settings and allowing two mismatches in the alignment. Identical read sequences mapping to the same loci were counted once per individual to reduce the potential impact of PCR duplicates on the counts. Variants' calls were obtained using the mpileup utility of SAMTools (<http://samtools.sourceforge.net/mpileup.shtml>) (Li *et al.*, 2009). Base Alignment Quality was used to score the variant calls and consensus calling was done using BCF tools. Maximum depth call was set at 8000. All variants were subjected to SNPlice. Cufflinks was used to assemble the transcripts without reference junction annotation; transcript abundance was quantified in fragments per kilobase per million (FPKM) fragments mapped, as previously described (Trapnell *et al.*, 2013). The variants were annotated using SeattleSeq Annotation Tools version 8.01, dbSNP build 138 (<http://snp.gs.washington.edu/SeattleSeq-Annotation138/>).

2.4 Computational algorithm

We developed a Python program, SNPlice, using the pysam Python module to find reads spanning SNV loci and exon-intron boundaries or exon-exon junctions (defined as spanning reads), and quantify the extent of co-occurrence of variant alleles in unspliced reads. The program identifies reads that span a SNV locus and an exon boundary within the length of the sequencing read, and classifies them according to the nucleotide observed at the SNV site (Supplementary Fig. S1). Reads are further required to extend past the exon-intron boundary by at least 5 bp to ensure the alignment can be confidently placed in the adjacent intron or in the following exon (Supplementary Fig. S2). The length of the alignment of each read to the reference is then checked—reads whose alignment length on the reference genome is similar (± 2 bp) to the length of the read are classified as intronic, while those whose alignment length on the reference genome is similar (± 2 bp) to the length of the read plus the length of the intron are classified as exonic. Reads whose nucleotide at the SNV position do not match either the reference or the alternative base, or whose alignment length does not match these intronic nor exonic definitions are disregarded, not because they are uninteresting, but because we must ensure the read counts are not inflated by false-positive or other types of poor alignments. For each SNV locus and exon-intron boundary, then, we compute four read counts (Fig. 1): N_{VARee} represents number of reads bearing the variant nucleotide and mapped across the exon-exon junction, N_{VARei} represents the number of reads bearing the variant nucleotide and mapped across the exon-intron boundary, N_{REFee} represents the number of reads bearing the reference nucleotide and mapped across the exon-exon junction, and N_{REFei} represents the number of reads bearing the reference nucleotide and mapped across the exon-intron boundary. We evaluate these counts in a 2×2 contingency table to assess the spliced versus unspliced status of variant versus reference allele reads. We compute the traditional log odds-ratio using pseudocounts of 0.5 to avoid numerical issues with zeros (Gart and

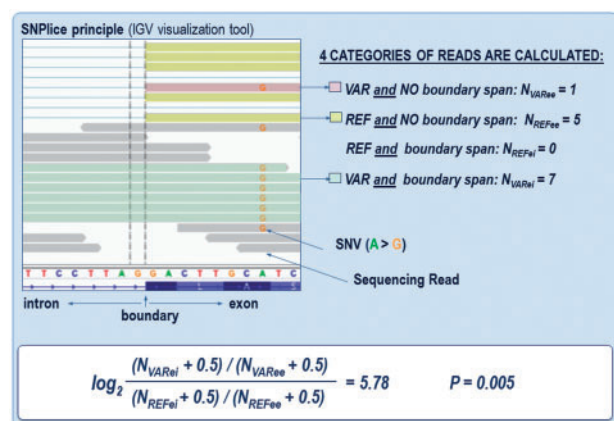


Fig. 1. SNPllice principle. Alignment of reads spanning a potential splice modulating SNV and an exon-intron boundary, illustrating the SNPllice analytical strategy. Sequencing reads with variant and reference nucleotide at the SNV position in the proximity of the boundary are shown (color coded). Variant-harboring reads often continue in the intron ($P = 0.005$), indicating association with potential junction alteration. The double vertical line indicates the first position of the intron

Zweifel, 1967; Haldane, 1955; Parzen *et al.*, 2002). The log odds-ratio increases as intronic reads become more enriched in variant allele reads. The statistical significance of the counts is determined using Fisher's exact test, which assesses the lack of independence in the observation of variant and intronic reads. Fisher's exact test P values were corrected for multiple trials by estimating the False Discovery Rate (FDR, Benjamini and Hochberg, 1995). SNVs of interest were visually examined through the Integrative Genome Viewer IGV (Thorvaldsdottir *et al.*, 2013).

SNPllice is freely available for download from <https://code.google.com/p/snpllice/> as a self-contained binary package and as python source code. SNPllice version 1.7.2 was used for the analyses described in this paper. The workflow is illustrated on Figure 2. Following analysis of raw reads using Tophat, and Samtools (mpileup utility), the resulting aligned reads (BAM format), junctions (BED format) and variants (VCF format) are read directly by SNPllice. Users can choose to include only annotated junctions through aligning the RNA-seq reads to the reference transcriptome. Prior to SNPllice, the variants can be annotated using SeattleSeq (VCF to VCF format)—all SNV annotations are retained in the SNPllice output. The analysis can be performed on reads from individual samples where observed heterozygous variants provide the basis for SNPllice analysis, or on pooled reads from many samples, making it possible to study the effect of the variants across heterozygous and homozygous samples.

2.5 Allele-specific Sanger sequencing

We designed allele-specific PCR, followed by Sanger sequencing, to illustrate the co-occurrence of variant nucleotide and exon-intron boundary for two of SNPllice highlighted loci. For each allele-specific PCR, three primers were designed: a common forward exonic primer to amplify the SNV locus, and two reverse primers hybridizing in the downstream exon or intron, respectively (Supplementary Table S2). First-strand cDNA was synthesized with SuperScript III reverse transcriptase (Invitrogen, Inc) using 1 μ g of total RNA and mixture of oligo dT primer and random hexamers. Two separate reactions, amplifying the region containing the SNV, and either the exon-exon junction, or exon-intron boundary, were performed in parallel using high fidelity LA Taq DNA polymerase

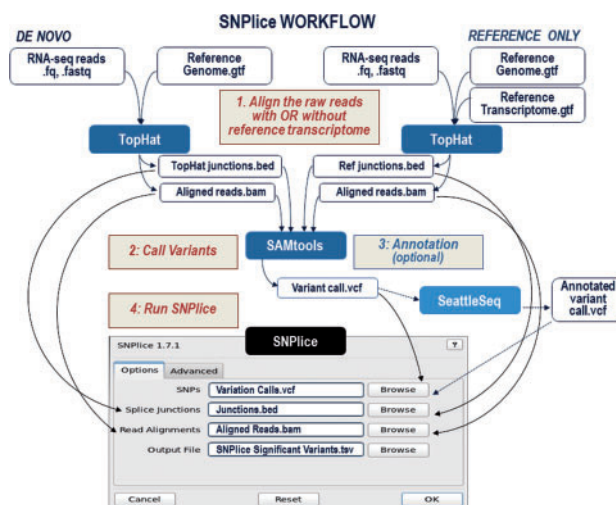


Fig. 2. SNPllice workflow. To analyze annotated junctions only, RNAseq reads can be aligned to the reference transcriptome

(Takara), according to the manufacturer recommendations. The products were gel-purified and subjected to bi-directional Sanger sequencing (ACGT Inc.), with the forward and the reverse primers used for the amplification.

3 Results

SNPllice processing of 65 human transcriptomes identified 141 unique variants significantly ($FDR < 0.05$) associated with intronic reads, 36 of which were observed in two or more unrelated samples (the 20 top-scored variants are shown in Supplementary Table S3). Between 0 and 18 variants were found per individual sample; this number positively correlated with the sequencing depth (Supplementary Fig. S3A). Comparison between the matched datasets revealed that 55% of the variants were called significant by SNPllice in both normal and tumor dataset; in all cases when the variant was called in only one of the dataset, this was the set with higher number of informative reads. We then compared the SNPllice significant calls across all samples heterozygous for the variant position (Supplementary Fig. S3B). Approximately one-third of the variants were called significant in all heterozygote samples in our datasets.

To assess SNPllice performance on pools of samples, we combined the read counts across the five RPE RNA-seq datasets and analyzed the summed counts using the same procedure as in SNPllice. This analysis identified 33 SNPllice significant variants, as compared to the 18 found through the individual analysis of the 5 datasets.

Of the 141 variants identified as significant by SNPllice in individual samples, 122 were positioned three and more nucleotides from the boundary of the exon. No correlation was seen between the distance of the variant to the splice site and the strength of the association. The most frequently observed nucleotide substitution (in regards to the sense orientation of the open reading frame) was C > T; in contrast, very few G > T and T > A substitutions were observed (Supplementary Fig. S3C). In regards to gene structure, 32% of the exonic SNVs were positioned in an in-frame exon, 14% in the first exon of the gene, 10% were in the last and 3% were within the 50 bp upstream of the last exon-exon junction (for at least one isoform). One SNV was a nonsense variant resulting in a

premature stop codon, 57 were missense substitutions and the rest were synonymous.

3.1 Assessment of splice-modulating potential of SNVs highlighted through SNPllice

Illustrative examples of SNPllice highlighted variants are listed in Table 1. Rs10749291 is a synonymous substitution in exon 4 of the gene *SFXN4* (c.258A > G, p.Q86Q, isoform ENST00000355697). IGV examination of the heterozygote sample confirmed the variant nucleotide only within reads encompassing the closest exon–intron junction, which was an acceptor site located six nucleotides from the SNV (Fig. 3A). Interestingly, the closest donor site (located 21 nucleotides from the SNV), was also encompassed almost exclusively by reads containing the variant nucleotide, leading to high proportion of molecules bearing the exon–intron junction on both sides of the exon ($P < 0.001$, Fisher's exact test). No reads bearing the reference nucleotide were mapped to the intron on either side of the exon. Next, we examined the homozygote samples for the reference and variant allele. Consistent with the lack of effect on the junction, the homozygous reference samples did not show any indication for alternatively spliced molecules (Fig. 3B). On the contrary, the homozygous variant samples showed a higher proportion ($P = 0.001$) of nonspliced reads than observed in the heterozygote sample (Fig. 3C). Thus, SNPllice identified a variant that confidently associates with junction alteration, in a manner consistent with allele-quantitative effect.

To assess the potential alternative transcript linked to rs10749291, we analyzed the assembly of the *SFXN4* gene generated by Cufflinks (Trapnell et al., 2010). Consistent with IGV examination, the assembly showed presence of an isoform retaining the introns and the further exons on both sides of exon 4 (Fig. 3D). The predicted open reading frame expands 50 codons downstream of exon 3 into intron 3, until it reaches an in-frame stop codon TAA (Supplementary Fig. S4). Despite being a predicted target of nonsense mediated mRNA decay (NMD), such an isoform has been isolated from multiple human tissues: (<http://www.ncbi.nlm.nih.gov/IEB/Research/Acembly/av.cgi?db=human&l=SFXN4.jAug10>). It is predicted to encode a protein of 134 amino acids that contains no characteristic *SFXN4* domain or trans-membrane motifs. Rs10749291 is a common variant (estimated minor allele frequency, MAF ~0.49) that has not been previously reported to associate with splicing alterations. Our data strongly suggest that rs10749291 is implicated in the generation of the above-described alternative *SFXN4* transcript. We next assessed the modulating potential of rs10749291 through splice-predictive tools. SplicePort estimated that the variant diminishes the acceptor strength, SpliceAid2 modeled that the change switches the binding site preference from the splice-regulator TIA-1 to PPT-binding protein PTB (Cavaloc et al., 1999; Caputi and Zahler, 2002; Jurica et al., 2002; Supplementary Fig. 5), and Skippy predicted gain of one new ESS (See Table 1).

Three more exonic variants scored by SNPllice as significant through individual sample analysis are presented in Table 1. Rs788023 is a C > T substitution located 7nt from the acceptor of exon 5 of *SF3B1* (Supplementary Fig. S6A). Analysis of the transcript assembly of *SF3B1* showed the presence of an isoform retaining the intron on the acceptor side of SNV-harboring exon, as well as the downstream positioned exon–intron–exon structure. *SF3B1* isoforms expressing intron 4 as a part of an alternative 5'-UTR are described, and predicted to encode a partial protein of 345 AA (<http://srv00.ibbe.cnr.it/ASPicDB/newresults.php?organism=human&cjob=list4830/job7596>). The second variant, rs12004, is situated

8 nt from the acceptor inside exon 4 of *KDELR3* (Supplementary Fig. 6B); the variant nucleotide is modeled to create a new binding site for the spliceosome component hnRNP K (Caputi and Zahler, 2002). Reads assembly from the same sample showed presence of an alternative known last exon of *KDELR3*, present in major protein-coding *KDELR3* isoforms (i.e. CCDS46705.1). The third SNV, rs11552262, is located 7 nt from the acceptor inside exon 2 of *TMEM129* (Supplementary Fig. S6C). This variant was predicted to switch the splice site from acceptor to donor, and to destroy one existing and create three new ESEs. Reads assembly in the region of rs11552262 showed very low expression (FPKM < 0.2) of an isoform with partial intron retention on the acceptor site of exon 2, that has not been described before.

The remaining two variants in Table 1, rs1140458 in *NPC1* and rs1131476 in *OAS1* reached statistical significance only after pooling the reads from the individual samples in the RPE dataset. Both variants were predicted through SplicePort to destroy existing canonical splice sites—donor for *NPC1*, and acceptor for *OAS1*. In addition, rs1140458 in *NPC1* was predicted to lead to loss of a binding site for the splice factor YB-1 (Ray et al., 2009), and loss of an exonic enhancer. We decided to further analyze these two variants through allele-specific Sanger sequencing.

3.2 Allele-specific Sanger sequencing of variant-boundary sites highlighted by SNPllice

To assess for the SNPllice suggested co-occurrence of variant nucleotide and exon–intron boundary, an AS-RT-PCR was designed to amplify in parallel the exon–exon junction, and the exon–intron boundary containing molecules (Supplementary Fig. S7A), for each of the two selected SNVs (rs1140458 in *NPC1* and rs1131476 in *OAS1*). The resulting Sanger sequencing chromatograms are shown on Supplementary Figures S7B and S7C, respectively. The chromatograms were examined for relative signal (peak) of the variant versus the reference peak in the exon–exon and the exon–intron amplicons. Ideally, to confirm association of variant nucleotide with intron-containing reads, we anticipate predominant presence of the variant signal (versus reference) in the chromatograms from the exon–intron product, while the reference would be retained in the canonically spliced exon–exon junction containing amplicons.

As seen on Supplementary Figures S7B and S7C, the sequencing confirmed the allele-specific junction alteration that was identified by SNPllice. The top chromatogram on Supplementary Figure 7B shows canonically spliced *NPC1* fragment (as indicated by the presence of an exon–exon junction between exons 18 and 19 of *NPC1*), and rs1140458 in heterozygous state, as indicated by equally strong signal from the reference and the variant base. In contrast, amplicons harboring the exon–intron boundary (second from the top chromatogram on Supplementary Fig. S7B) contained almost exclusively the variant nucleotide peak. The results were consistent with the reverse primer (Supplementary Fig. S7B, bottom chromatograms). Retaining of intron 19 donor sequence into the *NPC1* open reading frame is predicted to result in a stop codon generation immediately after the last codon of exon 18. A protein coding *NPC1* isoform terminated after exon 18 has been described (uc010xba, 766 AA, UCSC genes); our results suggest potential involvement of rs1140458 in the uc010xba formation.

Furthermore, even stronger association with junction alteration was detected for rs1131476 in *OAS1*. While the canonical splicing apparently tolerated molecules harboring the rs1140458 variant in *NPC1* (supported by presence of both reference and variant peak in

Table 1. SNVs located outside canonical splice-site sequences and assessed significant through SNPlice for association with intron retention. Comparative splice-altering potential is estimated through SplicePort (threshold = 1, FDR < 0.1), SpliceAid2, and Skippy. DTB = Distance to Boundary, A = acceptor, D = donor.

Chr:location (hg19)	REF/VAR	Rs#	Gene/exon	DTB (nt)	Ex size (nt)	P value	q (FDR)	SplicePort (A/D)		SpliceAid2			Skippy		ESS gain		
								REF	VAR	REF	factor		VAR	factor		ESE loss	ESE gain
											motif	factor					
10:120920588	T/C	10749291	SFXN4 ex4 (14)	6 (A) 21 (D)	27	0.0002 0.0007	0.03 0.05	A: 0.2 q < 0.001	A: 0.1 q = 0.012	aagaa aagaag agaag	SFRS10 TRA2A HNRNPH1 HNRNPH2 SFRS10 SFRS11 SFRS2	acagg aggaa	SFRS5 SFRS9	0 0	0 0	1	
2:198283305	T/C	788023	SF3B1 ex5 (25)	7 (A)	80	0.0001	0.03	A: 1.2 q < 0.001	-	gttttc	HUB TIA-1 TIAL1	tcttc	hnRNP (PTB)	0	4	0	
22:38877461	T/G	12004	KDELR3 ex4 (4)	8 (A)	253	0.001	0.05	A: -0.64 q = 0.057	A: -0.6 q = 0.053	-	-	tcctcat	hnRNP	0	0	0	
4:1720346	A/G	11552262	TMEM129 ex2 (4)	7 (A)	475	0.001	0.05	A: 1.47 q < 0.001	D: -0.9 q = 0.076	-	-	-	-	1	0	5	
18:21119777	C/T	1140458	NPC1 ex18 (25)	3 (D)	116	0.008	1.00	D:0.08 q = 0.01	-	acaac	YB-1	-	-	1	0	0	
12:113357209	G/A	1131476	OAS1 ex6 (6)	16 (A)	165	0.027	1.00	A:1.33 q < 0.001	-	-	-	-	-	0	0	0	

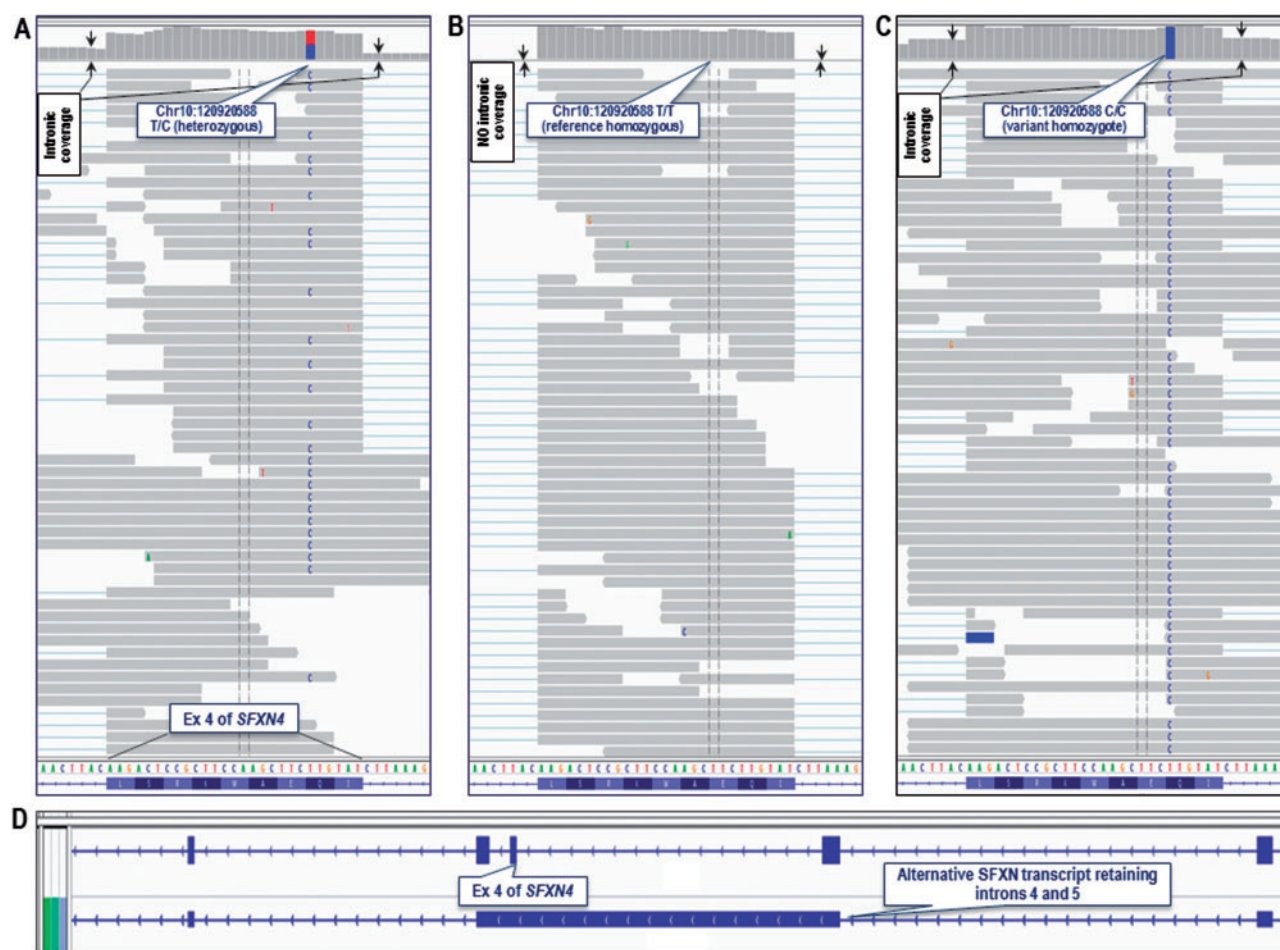


Fig. 3. Read alignment and assembly in the region of rs10749291. (A) Heterozygote sample: exclusive residing of the variant nucleotide within reads encompassing the exon-intron boundaries on both sides (located 6 and 21 nucleotides from the SNV), is seen. Read abundance shows relatively high proportion of intronic coverage on both sites of the boundary (arrows). (B) Homozygote reference sample: no reads are encompassing either one of the two boundaries, as also indicated by the complete absence of intronic coverage. (C) Homozygote variant sample: higher proportion of non-spliced reads, as compared to the heterozygote sample, supportive for allele-quantitative effect. (D) IGV visualization of the Cufflinks assembly (.gtf) showing the presence of an isoform retaining the introns on both sides of exon 4 of *SFXN4* (bottom track); the reference assembly is on the top. The gene orientation is indicated by arrows along the introns

the exon-exon amplicons on [Supplementary Fig. S7B](#)), *OAS1* alleles harboring rs1131476 variant nucleotide, were completely absent in the canonically spliced RNA product ([Supplementary Fig. S7C](#), top chromatogram). Similarly to the rs1140458 variant in *NPC1*, exon-intron harboring molecules were characterized by sole presence of the variant peak ([Supplementary Fig. S7C](#), second from the top chromatogram).

The results were consistent also with the reverse primer ([Supplementary Fig. S7C](#), bottom chromatograms). Visual examination of the proximal to rs1131476 sequences of *OAS1* identified the presence of closely positioned coallelic intronic variant, rs10774671, located in the canonical acceptor site. From the two in-phase variants, rs10774671 is more likely to be implicated in the junction alteration, due to its splice-site location. Without necessarily being involved in the underlying biological process, the coallelic rs1131476 is indicative of alternatively spliced *OAS1* alleles, and can potentially serve as a marker in association analyses. Rs1131476 and rs10774671 are located at the boundary between intron 5 and exon 6 of *OAS1* (ENST00000202917). An isoform expressing intron 5 as part of a 3'-UTR downstream of an alternative earlier *OAS1* last exon is described

(<http://www.ncbi.nlm.nih.gov/IEB/Research/Acembly/av.cgi?db=human&cl=OAS1.c-Aug10>). Whether the detected in our experiment intron-retaining RNA molecules are part of the described, or of a novel *OAS1* isoform, is subject of future investigations. Nevertheless, our data strongly suggest involvement of the rs1131476 and/or rs10774671 in the generation of an intron retaining expressed *OAS1* isoform. Rs1131476 and rs10774671 illustrate an important example where SNPlce highlights SNVs physically linked (in-phase) to other splice-altering features (such as SNVs positioned in splice-sites, See [Supplementary Fig. S7C](#)).

4 Discussion

Until recently, direct assessment of allelic phase for DNA and RNA features of diploid genomes has been possible mostly through molecular cloning. Next-generation sequencing technologies are based on the production of a nearly ideal copy of a single DNA or RNA molecular segment, commonly termed 'sequencing read'. Due to the uninterrupted process of template-based sequencing read generation, the features of the original molecule are preserved in the copy. As a consequence, molecular characteristics belonging to the same

molecule, such as variant nucleotide and exon–intron boundary, can be evaluated in their allelic corelationship, and tools utilizing this information have began to emerge (Viner *et al.*, 2014). SNPlce utilizes the allele-specific signal available in the massively parallel sequencing platforms to assess co-occurrence between variant nucleotide and nearby exon–intron boundaries. Hence, SNPlce highlights variants preferentially occurring on intron-containing molecules, possibly resulting from altered splicing. In addition, SNPlce considers paired-end sequencing reads, making it possible to assess longer distance variant-effected splicing. IGV examination of highlighted loci showed consistent with SNPlce co-occurrence of variants and junctions, which was further illustrated through allele-specific Sanger sequencing. Thus, SNPlce provides useful means for screening of transcriptome reads to identify novel splice altering variants, and to assess the splice-altering potential of splice-site positioned substitutions. Furthermore, SNPlce analysis of RNA-seq datasets from diseased tissues can identify rare pathogenic variants that are currently considered neutral due to lack of evidence for effect on the protein function. Finally, comparing SNPlce findings between groups of patients and controls could identify disease-implicated splicing deregulation.

Applying SNPlce, we were able to identify variants that selectively reside in alternatively spliced RNA molecules; the harboring motifs are to be submitted to SpliceAid-F (Giulietti *et al.*, 2013). Cufflinks assembly of the reads in the SNV region suggested expression of alternative isoforms, in some cases, expressed at protein level. Most of these isoforms have been previously annotated through independent experiments, thus supporting the expression of the intron-retaining RNA molecules identified in our study. However, the described SNVs have never been directly linked to the expression of these particular isoforms. In this regard, SNPlce offers an experimentally based tool to identify novel relationships between encoded and expressed genomic layers.

Relatively few splice-site positioned variants (i.e. within the two nucleotides immediate to the boundary) were scored significant through SNPlce. This is not surprising, as many variants with strong effect on the splicing are expected to be eliminated through the evolutionary selection. One additional explanation is that, if the junction alteration creates a frame-shift, molecules bearing the alternative junction and the variant nucleotide may be degraded through nonsense-mediated mRNA decay (NMD). While this is expected to eliminate or reduce the number of variant-bearing reads, such an effect is difficult to assess using RNA data alone. However, splice-modulating variants that lead to NMD can be detected through SNPlce assessment of cell cultures under experimentally inhibited NMD.

Currently, the genome-scale splice-modulating potential of SNVs is estimated mostly through modeling tools built on knowledge derived from gene- or variant-focused experiments. Comparative analysis of selected significant variants from SNPlce results through SplicePort, SpliceAid2 and SkipPy, were concordant with at least one of the three tools. Some variants, however, did not seem to affect known donors or acceptors, or to alter known binding motif or ESE. Because SNPlce assesses empirically derived data, it may highlight variants acting through unknown mechanisms, which are not currently implemented in the predictive pipelines.

Individual SNPlce assessment of the transcriptomes in our dataset identified between 0 and 18 heterozygous variants per sample associated with junction alteration at false discovery threshold 0.05. Because the statistical analyses are based on transcriptome sequencing read counts, the computed values are linked to the coverage (resp. expression levels) at the particular locus. Therefore, for

many loci, strong statistical significance is unlikely to be reached due to relatively low number of reads, which can also explain the incomplete consistency between the matching normal and tumor dataset. For example, the two wet-lab validated SNVs reached significance only through pooled analysis, and not in any individual sample. An approach to address low read number is to combine the read counts from multiple samples to be processed through SNPlce as a whole. As illustrated, the combined approach increased the number of significant SNVs, at the same time retaining most of the variants identified through the individual analysis. An additional inherent advantage of the combined approach is that it considers the reads from homozygote samples, thus increasing the count of informative reads. This is especially applicable to intronic variants, which, if exerting a strong effect on splicing, naturally tend to appear as mono-allelic expression in the transcriptome (see Supplementary Fig. S7C). However, pooling reads from different samples needs to be applied with caution, as it assumes identical splicing regulation, and eliminates the uniqueness of splice factors and conditions that may be directly linked to the involvement of the particular variant in the splice alteration.

An inherent advantage of SNPlce is its immediate link to the empirical data. As the perspective on splicing turns into highly dynamic, condition-specific mechanism, SNPlce is poised to support cell- and tissue-specific analyses through individual transcriptome assessment, as well as to study dynamic, pathogenic and developmental splicing patterns. In addition, since cells typically coordinate numerous changes in ‘splicing programs’ (Braunschweig *et al.*, 2013) analyzing the whole transcriptome can capture splice changes in their mutual dependencies. Finally, being based on read counts, SNPlce provides means for quantitative estimations of the splice changes across multiple samples. Application of the pipeline to large-scale datasets is expected to reveal multiple new splice modulating SNVs, which in turn, may highlight novel splice regulatory mechanisms or disease implicated genetic changes. In addition, SNPlce provides an innovative strategy to re-visit the splice-modulating potential of SNVs located in canonical sequences that are traditionally considered critical for splicing regulation.

Funding

This work is supported by MGPC, GWU; NIH National Center for Advancing Translational Sciences [UL1TR000075]; Clinical and Translational Science Institute at Children’s National Medical Center [CTSI-CN to A.H.]; and the Georgetown University Dean’s Pilot [GX4002-753 to N.G.].

References

- Barash, Y. *et al.* (2010) Deciphering the splicing code. *Nature*, **465**, 53–59.
- Barbosa-Morais, N.L. *et al.* (2012) The evolutionary landscape of alternative splicing in vertebrate species. *Science*, **338**, 1587–1593.
- Benjamini, Y.H. and Hochberg, Y. (1995) Controlling the false discovery rate: a practical and powerful approach to multiple testing. *J. R. Statist. Soc. B*, **57**, 289–300.
- Bernstein, B.E., *et al.* (2012) An integrated encyclopedia of DNA elements in the human genome. *Nature*, **489**, 57–74.
- Braunschweig, U., *et al.* (2013) Dynamic integration of splicing within gene regulatory pathways. *Cell*, **152**, 1252–1269.
- Brendel, V. and Kleffe, J. (1998) Prediction of locally optimal splice sites in plant pre-mRNA with applications to gene identification in Arabidopsis thaliana genomic DNA. *Nucleic Acids Res.*, **26**, 4748–4757.
- Brunak, S., *et al.* (1991) Prediction of human mRNA donor and acceptor sites from the DNA sequence. *J. Mol. Biol.*, **220**, 49–65.

- Caputi, M. and Zahler, A.M. (2002) SR proteins and hnRNP H regulate the splicing of the HIV-1 *tev*-specific exon 6D. *EMBO J.*, **21**, 845–855.
- Cavaloc, Y. et al. (1999) The splicing factors 9G8 and SRp20 transactivate splicing through different and specific enhancers. *RNA*, **5**, 468–483.
- Cheung, V.G. et al. (2005) Mapping determinants of human gene expression by regional and genome-wide association. *Nature*, **437**, 1365–1369.
- Clark, F. and Thanaraj, T.A. (2002) Categorization and characterization of transcript-confirmed constitutively and alternatively spliced introns and exons from human. *Hum. Mol. Genet.*, **11**, 451–464.
- Coulombe-Huntington, J. et al. (2009) Fine-scale variation and genetic determinants of alternative splicing across individuals. *PLoS Genet.*, **5**, e1000766.
- De Conti, L., et al. (2013) Exon and intron definition in pre-mRNA splicing. *Wiley Interdiscip Rev RNA*, **4**, 49–60.
- Dogan, R.I., et al. (2007) SplicePort—an interactive splice-site analysis tool. *Nucleic Acids Res.*, **35**, W285–291.
- ElSharawy, A. et al. (2006) SNPSplicer: systematic analysis of SNP-dependent splicing in genotyped cDNAs. *Hum. Mutat.*, **27**, 1129–1134.
- ElSharawy, A. et al. (2009) Systematic evaluation of the effect of common SNPs on pre-mRNA splicing. *Hum. Mutat.*, **30**, 625–632.
- Faber, K., et al. (2011) Genome-wide prediction of splice-modifying SNPs in human genes using a new analysis pipeline called AASites. *BMC Bioinformatics*, **12** (Suppl. 4), S2.
- Gart, J.J., and Zweifel, R. J. (1967) On the bias of various estimators of the logit and its variance with application to quantal bioassay. *Biometrika*, **54**, 181–187.
- Giulietti, M. et al. (2013) SpliceAid-F: a database of human splicing factors and their RNA-binding sites. *Nucleic Acids Res.*, **41**, D125–D131.
- Haldane, J.B.S. (1955) The estimation and significance of the logarithm of a ratio frequencies. *Ann. Hum. Genet.*, **20**, 309–311.
- Han, H. et al. (2013) MBNL proteins repress ES-cell-specific alternative splicing and reprogramming. *Nature*, **498**, 241–245.
- Hull, J. et al. (2007) Identification of common genetic variation that modulates alternative splicing. *PLoS Genet.*, **3**, e99.
- Jurica, M.S. et al. (2002) Purification and characterization of native spliceosomes suitable for three-dimensional structural analysis. *Rna*, **8**, 426–439.
- Kamath, U. et al. (2012) An evolutionary algorithm approach for feature generation from sequence data and its application to DNA splice site prediction. *IEEE/ACM Trans. Comput. Biol. Bioinform.*, **9**, 1387–1398.
- Kim, D.P. et al. (2013) TopHat2: accurate alignment of transcriptomes in the presence of insertions, deletions and gene fusions. *Genome Biol.*, **14**, R36.
- Li, H. et al. (2009) The Sequence Alignment/Map format and SAMtools. *Bioinformatics*, **25**, 2078–2079.
- Liao, P.Y. et al. (2005) Splicing for alternative structures of Cav1.2 Ca²⁺ channels in cardiac and smooth muscles. *Cardiovasc. Res.*, **68**, 197–203.
- Maminishkis, A., et al. (2006) Confluent monolayers of cultured human fetal retinal pigment epithelium exhibit morphology and physiology of native tissue. *Invest Ophthalmol. Vis. Sci.*, **47**, 3612–3624.
- McManus, C.J. and Graveley, B.R. (2011) RNA structure and the mechanisms of alternative splicing. *Curr. Opin. Genet. Dev.*, **21**, 373–379.
- Merkin, J. et al. (2012) Evolutionary dynamics of gene and isoform regulation in Mammalian tissues. *Science*, **338**, 1593–1599.
- Moore, M.J. and Silver, P.A. (2008) Global analysis of mRNA splicing. *RNA*, **14**, 197–203.
- Pan, Q. et al. (2008) *Nat. Genet.*, **40**, 1413–1415.
- Parzen, M. et al. (2002) An estimate of the Odds Ratio that always exists. *J. Comput. Graphical Stat.*, **11**, 420–436.
- Perte, M. et al. (2001) GeneSplicer: a new computational method for splice site prediction. *Nucleic Acids Res.*, **29**, 1185–1190.
- Piva, F. et al. (2012) SpliceAid 2: a database of human splicing factors expression data and RNA target motifs. *Hum. Mutat.*, **33**, 81–85.
- Ray, D. et al. (2009) Rapid and systematic analysis of the RNA recognition specificities of RNA-binding proteins. *Nat. Biotechnol.*, **27**, 667–670.
- Riva, A. (2012) Large-scale computational identification of regulatory SNPs with rSNP-MAPPER. *BMC Genomics*, **13** (Suppl 4), S7.
- Singh, R.K. and Cooper, T.A. (2012) Pre-mRNA splicing in disease and therapeutics. *Trends Mol. Med.*, **18**, 472–482.
- Sterne-Weiler, T. and Sanford, J.R. (2014) Exon identity crisis: disease-causing mutations that disrupt the splicing code. *Genome Biol.*, **15**, 201.
- Thorvaldsdóttir, H. et al. (2013) Integrative Genomics Viewer (IGV): high-performance genomics data visualization and exploration. *Brief Bioinform.*, **14**, 178–192.
- Trapnell, C. et al. (2010) Transcript assembly and quantification by RNA-Seq reveals unannotated transcripts and isoform switching during cell differentiation. *Nat. Biotechnol.*, **28**, 511–515.
- Viner, C. et al. (2014) Validation of predicted mRNA splicing mutations using high-throughput transcriptome data. Version 2. F1000Res. eCollection (<http://f1000r.es/378>).
- Wang, Z. and Burge, C.B. (2008) Splicing regulation: from a parts list of regulatory elements to an integrated splicing code. *RNA*, **14**, 802–813.
- Woolfe, A. et al. (2010) Genomic features defining exonic variants that modulate splicing. *Genome Biol.*, **11**, R20.
- Yeo, G. and Burge, C.B. (2004) Maximum entropy modeling of short sequence motifs with applications to RNA splicing signals. *J. Comput. Biol.*, **11**, 377–394.